A Multiwavelength Photometric Study of open star cluster NGC 1931

(27th May 2013 - 24th July 2013)

By: Abhijeet Anand

BS (1st year)

Indian Institute of Science, Bangalore

At

Aryabhatta Research Institute of Observational Sciences, Nainital

Under the supervision of

Dr. Saurabh Sharma

Scientist C

ARIES, Nainital

Abstract

A multi-wavelength photometric study of open young star cluster NGC 1931 was carried out during the month of June 2013 and their analysis and results are presented in detail. The aim of study is to carry out a deep CCD photometry and to find the interstellar reddening, age and distance of this young open star cluster NGC 1931 and correlate these results with previous obtained results.

The data used for the study and analysis are taken from the 104-cm Sampurnanand optical Telescope at ARIES, Nainital and all the basic parameters have been estimated by doing a deep photometric analysis of these data. Using Color-Magnitude diagram for the cluster the distance modulus, distance and age of cluster have been estimated as 13.65±0.32 mag, 2.31±0.34 kpc and 1-2 Myr respectively which are in good agreement with previous studies. The Color-Magnitude diagram clearly shows that this is a young open star cluster as most of the stars (even most massive ones) lie on the main sequence line of the diagram. Also the Color-Color diagram shows variable interstellar reddening with $E(B-V)_{\mathbf{min}}$ and $E(B-V)_{\mathbf{max}}$ as 0.59 ±0.04 mag to 0.96±0.05 mag (may be due to the presence of small nebula Sh2-237). It shows that may be young hot stars are still embedded in the molecular cloud of nebula.

1 Introduction

1.1 Open Star Clusters

The night sky is full of tiny twinkling dots which are found may be in large or small groups (called clusters) or isolated. Our own galaxy Milky Way consists of approximately 100- 400 billion [1] stars. Galileo Galilei (1564-1642) was perhaps been the first person who observed the group of stars (Open star clusters) through an optical telescope and believed that every nebula in the sky could be resolved into individual stars. In his opinion, the Galaxy consisted of stars grouped together in individual clusters.

Open clusters are small group of stars in terms of number of member stars (typically few dozen to few thousands of stars) and sizes (1-20 pc in diameter) with a little symmetry in appearances and diffuse morphology. Recent near IR surveys (Stauffer et al.2007)[2] are showing more members than we had previously thought in many clusters. Since they generally lie in galactic plane therefore they are also known as *Galactic Clusters*. They are generally found in spiral and irregular galaxies in which active star formation is occurring and are loosely bound to each other by mutual gravitational attraction. They are easily differentiated from background (or foreground) stars because of their symmetrical appearances. The ages generally lie between few Myr to the age of galaxy. It was assumed that all members in cluster are coeval but recent studies [3] show the presence of age range among the members of young open clusters. Young open clusters are often associated with interstellar cloud and they usually contain bright main sequence stars, blue super-giants, and sometimes a few variable stars, either young Cepheids (class of very luminous variable stars) or even younger pre main sequence (PMS) T Tauri type stars. A catalogue by W.S. Dias[4] list 2174 open clusters. Since their stellar density is not so high (~0.1-10 stars/pc^3) because of loosely bounded by weak gravitational interaction among them and they are generally located in galactic plane so due to the differential rotation of galactic disk clusters towards the central part of galactic disk do suffer a lot of collision and survive for few hundred million years, Consequently only a few clusters survive to a very old age; Till now the oldest identified clusters are about 9 Giga years

old (Berkeley 17, NGC 6791; Salaris et al.2004 [5]) which are usually found in outer part of the galactic disk where they suffer a less amount of collision [6] with galactic materials and survive for long duration. As they are members of galactic disk they are metal rich and represent the population of its stars.

1.2 Importance of Open Star Clusters

Since it is believed that majority of stars in our galaxy form in groups (clusters) therefore open clusters have been the excellent universal laboratories for the study of Star formation, stellar evolution and their properties. Today astronomers have an intense understanding of origin and physical properties of open clusters. The extensive studies of clusters have contributed tremendously in understanding the structure and evolution of the Galaxy as well as different stages of the stellar evolution because of the following properties; all the stars in cluster are at same distance because of mutual gravitational interaction which holds the member stars within a small region (1-20 pc), it is often assumed that they all have the same age and chemical composition and differ only in their masses and types. These properties allow us to draw constant loci of age and composition in many diagrams. As with the time age vary, it fetches a lot of information regarding the age of galaxy and stars. Young open clusters provide us the information of current star formation processes, unveil the mysteries of galactic structure because they are loosely bound and less than 10 Myr in age.

1.3 NGC 1931

NGC 1931 is a young open star cluster associated with gas-dust complex and the bright nebula Sh2-237 in Auriga constellation of our galaxy [7]. It is a *Galactic Cluster* as the latitude shows ($\ell = 0.28$) that it lies in galactic plane. The distance of cluster is variable between 1.8 kpc to 3.1 kpc (Moffat et al.1979 [8]) as E(B-V) is variable in that region. The recent study [7] reveals two clustering in region and differing reddening law in the

region. The entire cluster is only about 3 arcmin[9] in size. The post main sequence age of cluster has been reported as ~10 Myr[8],[10], and mean age of Young Stellar Objects(YSOs) are 2-3 Myr [7]. It is also considered as miniature version of nebula Orion due to its similar properties with nebula. Table 1.1 gives the basic parameters for NGC 1931.

Table 1.1

Parameters for NGC 1931

Parameters	*Value*	*Reference*
Sky Coordinates	RA= $05^{h}\ 31^{m}\ 25^{s}$, Dec = $+34^{\circ}\ 14'\ 42''$	SIMBAD (J2000)
Galactic Coordinates	$\ell=173.9^{o}, b=0.28^{o}$	SIMBAD (J2000)
Distance	≈ 2.3 kpc	[7]
Age	2-3 Myr (for YSOs) and ~10Myr (for Post main sequence stars)	[7],[8],[10]

Although the object has been studied very extensively in past but some detailed spectroscopic studies have not been done yet, which could provide some very accurate data for their basic parameters such as identification of cluster membership and Initial Mass Function (IMF) of the cluster. Also the photometric and polarimetric studies [7] of NGC 1931 show the triggered star formation in the region.

1.4 Objectives

The present study aims to estimate the basic parameters (like age, distance, interstellar reddening, and extinction coefficients for all five bands i.e. U, B, V, I, R with further accuracy and to see the consistency with previous determined values[7], [8], [10]. Also the Color-Magnitude diagram clearly shows us that most of the massive members of the cluster are on the main sequence along with the presence of YSOs in Pre-main

sequence (PMS). The Color-Color diagram reveals variable interstellar reddening (0.59 to 0.96).

2 Data Reduction Techniques

2.1 Data Acquisition

All the raw data(multiple images for both standard field SA98 and cluster NGC 1931)were taken from 104 cm(primary mirror diameter) Sampurnanand telescope in a single night with different exposure times in different bands (U, B, V, R, I). The telescope uses Wrights (2k) 2048 x 2048 CCD with 24 micron pixel size, and 15-bit ADU as detector and Johnson and Morgan UBV and Kron-Cousins RI filters with a mean wavelength of 375 nm, 430 nm, 530 nm, 641 nm and 798 nm for U, B, V, R and I respectively and bandwidth (width of range of frequencies) for U, B, V, R, and I are 60 nm, 110 nm, 90 nm, 138 nm and 110nm respectively. The following sections will describe the data reduction and analysis of observations.

2.2 CCD Data Reduction Techniques

The basic operation of data reduction generally involves the mathematical manipulation (like addition, subtraction, multiplication or division) of frame by another frame to correct all the instrumental and physical errors while taking the CCD (Charge-Coupled Devices) raw images. For all these purposes several software packages have been developed by different astronomical observatories like IRAF and DAOPHOT by NOAO (National Optical Astronomy Observatory, USA) and DAO (Dominion Astrophysical Observatory, Canada). The whole basic stages of image processing can be summarized in the form of a chart given in fig 1.

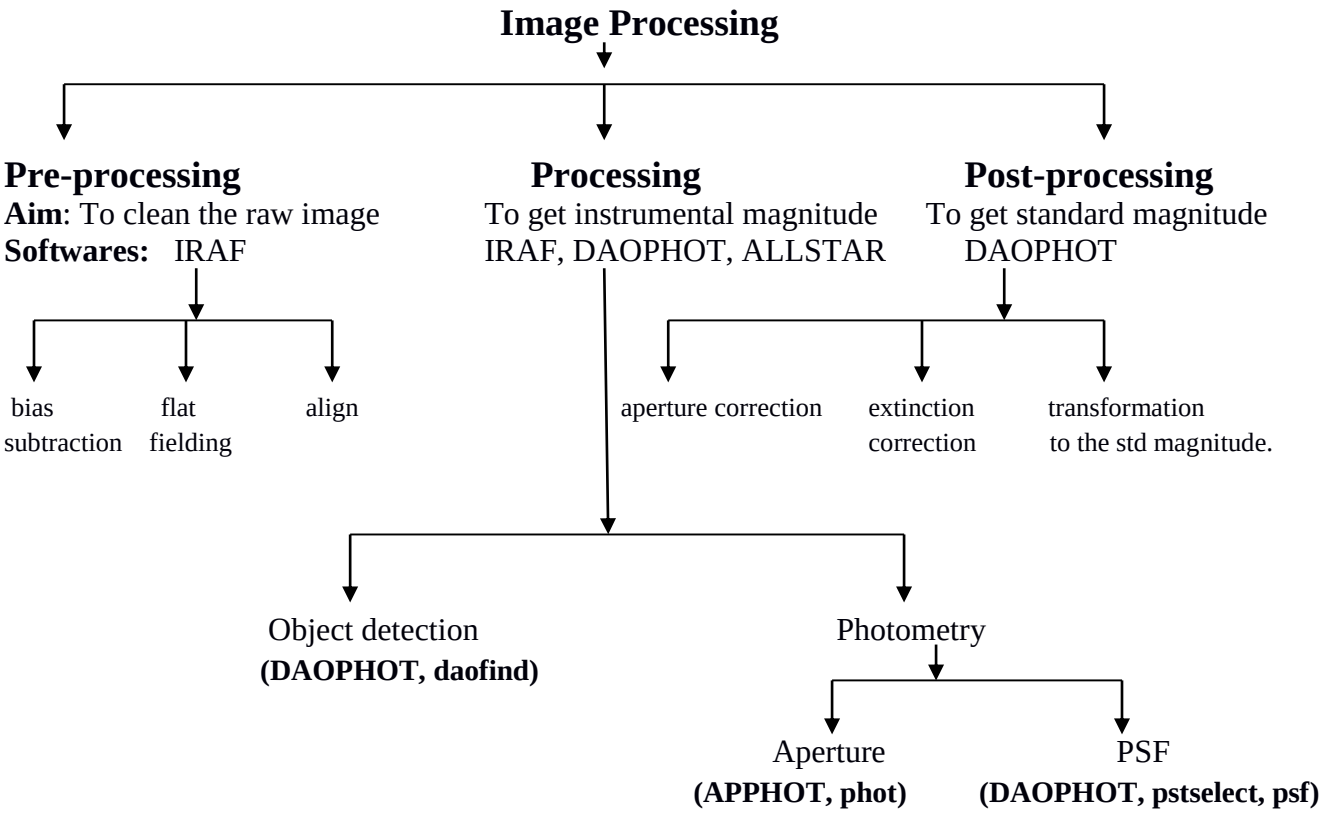

Fig 1: Chart summarizing the complete process of Image processing and Photometry

2.2.1 Image Processing

2.2.1.1 Pre Processing

To analyze the properties and use it to estimate the basic parameters of a system we first must have to clean all the raw CCD images, which involves following stages.

I. Bias Subtraction

There is always a d-c offset associated with CCD to provide the best possible ADU value for incoming star counts (photons), but this is an instrumental error which must be corrected before proceeding our object observation, so for this purpose several frames are taken when the CCD shutter is closed and then using IRAF software package an average frame of those frames is developed, which is subtracted from all the frames as initial correction. To perform this task IRAF's **"noao"** package is used

in which task **ccdred** and **zerocombine** were used.

II. Flat Fielding

Since CCD is made of very tiny (μm size) squares known as pixels is very sensitive to incoming photons but due to manufacturing errors sensitivity for every pixel is not same due to which resulting images present spatial noise (i.e. photo response non-uniformity) which is corrected by acquiring frames (flat field images) made on uniform sky background and developed a median combined frame of all these flat images in different bands separately and then dividing our target images by this normalized master flat image we finally clean our target images. To perform this task **ccdred** and **flatcombine** tasks were used.

III. Align and Combine

To find our object in different bands and perform photometry we must align our all images with reference to a fixed image (based on our own choice). Then to increase signal-to-noise (S/N) ratio all the frames (long exposure images) are combined separately in all different bands (U, B, V, R, I). For these purposes in **apphot** package **center**, **imalign** and **imcombine** tasks were used.

2.2.1.2 Processing

After doing all corrections in pre-processing we finally get a clean and aligned image which further would be used to determine the positions and instrumental magnitude of the stars which is known as "Photometry". The following steps are involved in these processes.

I. Object Detection

First of all it is the most significant task to know our desired objects (here stars) in images because it would definitely contain undesired things (like cosmic rays, foreground and background stars). Since our field is so crowded therefore we used DAOPHOT package of IRAF in which there is a task called **"daofind"** which automatically detects star like objects based on the data of mean sky, FWHM (full width half maximum), and sky sigma values of that image. To select mostly desired objects we kept sigma value 4 in all bands.

II. Photometry

It is the process by which we obtain numerical values of brightness of the stars in units of magnitude. We have performed two basic procedures for obtaining quantitative magnitudes of the stars obtained in **daofind** file. The two basic procedures are: Aperture Photometry and Point Spread Function (PSF) photometry using IRAF software package.

- **Aperture Photometry**

Aperture magnitude give us the brightness of a star in terms of magnitude which is based on the counts of a star absorbed in CCD pixels. To estimate this magnitude in aperture photometry the counts in a given box (generally a circle as it is assumed that stars are point sources of light) centered on that star are integrated and the counts in an equal area near the vicinity of the star (star free area) are subtracted from the former. This gives the resulting counts for that particular star which is further converted into magnitude easily. The method can easily be understood by fig 2.

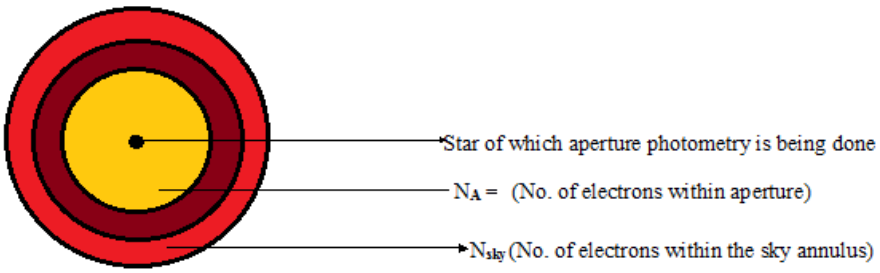

Fig: 2

The mathematical formulation used for the calculation of counts of star is as follows:

$$N_* = N_A - \left[\frac{N_{sky}}{A_{sky}}\right] \cdot A \qquad \text{---(3)}$$

Where A_{sky} = Area of sky annulus)
A = Area of Aperture for which magnitude is being calculated.
N_* = No. of electrons for star

Then by using following equation aperture magnitude is calculated generally

$$m_A = -2.5 \cdot \log_{10} N_* + c \qquad \text{---(2)}$$

Where, c = zero point (IRAF keeps it 25 by default).

Aperture Magnitudes were calculated for standard field **SA98** in all bands using **phot** task in **apphot** package of IRAF. Magnitudes were calculated at two aperture radii i.e. 1·FWHM and 4·FWHM because the star counts do mathematically maintain a Gaussian curve for random distribution for every star so approximately 99% counts were covered till 4·FWHM aperture radius. IRAF used following algorithm to estimate the numerical value of aperture magnitude. Using equation (1) it first calculates the flux for star within that aperture and then using equation (3) it estimates the aperture magnitude.

$$m_A = -2.5 \cdot \log_{10}(N_*) + 2.5 \cdot \log_{10}(t) + c \qquad \text{---(3)}$$

Where t = Exposure time for each frame, c = zero point (i.e. 25 for IRAF by default)

- **Point Spread Function (PSF) Photometry**

Aperture photometry is the best method to find accurate quantitative values for brightness of stars in terms of magnitude but it works well with uncrowded field so that in given aperture no other stars (i.e. contamination) should come. In aperture photometry of crowded field if more than one star come within the same aperture it will give an increased magnitude for star with errors. But since our field NGC 1931 was a crowded field (as it is an open star cluster) therefore we performed IRAF's PSF

photometry for each star. In a crowded field even for well separated stars bright stars can shadow faint neighbours. For doing PSF we used DAOPHOT package in IRAF. The tasks **pstselect, psf** and **allstar** were used to perform PSF photometry of NGC 1931. We used Gaussian fit for our PSF. For PSF photometry IRAF fits a Gaussian profile for some selected stars (i.e. the analytic function is integrated over the area of pixel and a correction factor is estimated by a bicubic interpolation of star counts and added to the integral and magnitude is calculated). First of all **pstselect** and **psf** task this photometry for a fixed number of stars and using **allstar** task this profile fitting is applied to all the stars. Mathematically a Gaussian profile is given by,

$$f(x) = A \cdot e^{-(\frac{r^2}{2a^2})}$$

Where A= PSF profile fitting constant

r = PSF radius, which we kept 4·FWHM

a = fitting parameters.

Finally we got PSF magnitudes for all stars which we corrected by adding the average difference of magnitudes for some selected bright isolated stars as follows to bring it on the level of aperture photometry.

Correction factor = Aperture Magnitude at 4·FWHM – PSF magnitude (at 4·FWHM)
Corrected PSF mag. = PSF mag. + Correction factor

Here it is important to note that the correction factor itself was a negative value so this decreased the magnitude of all stars including fainter ones which we wanted.

2.2.1.3 Post Processing

I.Aperture Correction

After calculating the magnitudes for both the aperture radii we performed the aperture correction for the counts that were left out in the estimation of sky annulus and aperture area. To correct these errors we calculated the difference of magnitudes at

both aperture radii for several bright and isolated stars and applied it to the magnitudes calculated at 1·FWHM. This was done by a file reading program in C language.

Correction factor = Magnitude at 4·FWHM – Magnitude at 1·FWHM

m_C *= Magnitude at 1·FWHM + Correction factor*

Here it is important to note that the correction factor itself was a negative value so this decreased the magnitude of all stars including fainter ones which we wanted.

II.Extinction Coefficient

Whenever light travels from medium the medium absorbs some amount of light because of its particles due to which we do not get exact amount of photons which are emitted through a source and this reduces the intensity of light. As per the advanced laws for refractive index intensity of light falls exponentially for a medium which can be given as following

$$I = I_o e^{-d_1 \cdot x} \qquad \text{---(4)}$$

Where I = Intensity at any point other than the source

I_o = Intensity of light emitted through source.

x = Air mass, d_1 = constant

If we take log both side and using an empirical formula of reference magnitude in astronomy we would get

$$m_C = m_i + k \cdot x \qquad \text{---(5)}$$

Where $\boldsymbol{k}$ = Extinction Coefficient

$\boldsymbol{x}$ = Air mass of the image

m_C = Corrected aperture magnitude

m_i = Instrumental magnitude

Since refractive index depends on frequency so extinction coefficient is also dependent on frequency therefore we get different values of extinction coefficient for different bands. The extinction coefficient used in eqn. 5 is first order extinction coefficient which varies night to night because of variable earth's atmosphere. To

calculate these values we drew graph of air mass versus corrected magnitude for a single bright star in every frame in different bands. The values for extinction coefficient, we got for different bands have been shown in Table 2.1.

Table 2.1

Bands	*Extinction Coefficients*
U	0.545 ± 0.016
B	0.33 ± 0.022
V	0.184 ± 0.02
R	0.15 ± 0.02
I	0.11 ± 0.002

All these values are in good agreement with previous studies [7] and general values.

III.Calibration and Standardisation of Aperture Magnitudes

The magnitudes (for **SA98**) we got from IRAF were not standard so they had been first calibrated and then standardised which further used to find standard magnitudes for all the stars of NGC 1931 of which PSF photometry was performed. For this purpose first of all instrumental magnitudes for all the stars were estimated using eqn. 5. Then after using standard magnitudes of selected stars of **SA98** from **Landolt Standard Equatorial** [11] catalogue we drew the following graphs and using slopes and intercepts we calculated the standard magnitudes for all stars.

$$B_o - V_o = m_1 \cdot (B_i - V_i) + c_1 \qquad \text{---(6)}$$

$$U_o - B_o = m_2 \cdot (U_i - B_i) + c_2 \qquad \text{---(7)}$$

$$V_o - I_o = m_3 \cdot (V_i - I_i) + c_3 \qquad \text{---(8)}$$

$$V_o = V_i + m_4 \cdot (V_i - I_i) + c_4 \qquad \text{---(9)}$$

Where B_o, V_o, and U_o are the standard magnitudes for *B, V,* and *U* bands respectively and B_i, V_i, and U_i are instrumental magnitudes for *B, V,* and *U* bands respectively. m_1, m_2, m_3, m_4, and c_1, c_2, c_3, c_4 are slopes and intercepts for best fit straight line in Origin. The values for these constants are summarized in Table 2.2.

Table 2.2

Slopes	*Intercepts*
$m_1 = 0.986 \pm 0.01$	-0.22 ± 0.02
$m_2 = 0.972 \pm 0.01$	-2.02 ± 0.04
$m_3 = 0.98 \pm 0.009$	0.59 ± 0.007
$m_4 = 0.049 \pm 0.01$	-3.89 ± 0.01

IV.PSF Calibrations and Standardisation

Using eqn. (5) for PSF magnitudes we calculated instrumental PSF magnitudes, And then finally using our previously got values of m_1, m_2, m_3, m_4, and c_1, c_2, c_3, c_4 and applying equations (6), (7), (8), and (9) we standardised PSF magnitudes for stars of NGC 1931.

3 Analysis

3.1 Interstellar Reddening and Extinction

Extensive studies of dust particles (atoms, molecules or ions) of Interstellar medium (ISM) of our host galaxy (i.e. Milky Way) explained the interstellar reddening. They are revealing the fact that the typical size of dust grains are of the order of wavelength of blue light due to which when beam of photons travels through the medium the blue ones suffer maximum scattering due to which a very less amount of blue photons reach us and object appears redder than it originally is. This phenomenon of reddening of an object is termed as “Interstellar Reddening”. In astronomy it is a very important

task to determine this value because it gives us the accurate distance of the object. The scattering of light can easily be understood by fig 3 and fig 4.

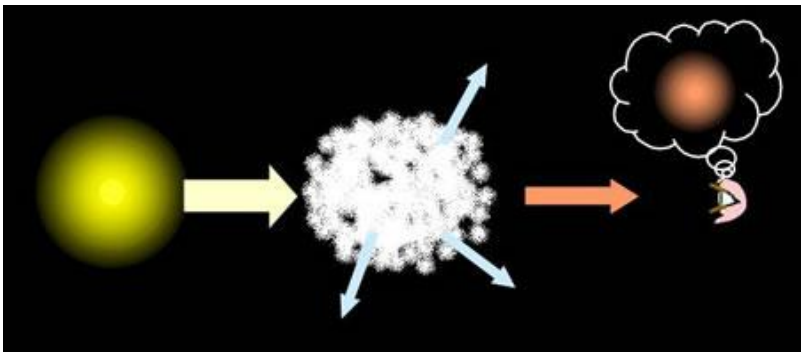

Dust grains along the line of sight scatter and absorb light coming from distant objects. We therefore see these objects as dimmer as and redder than they really are. These effects are known as extinction and interstellar reddening respectively.

Fig. 3

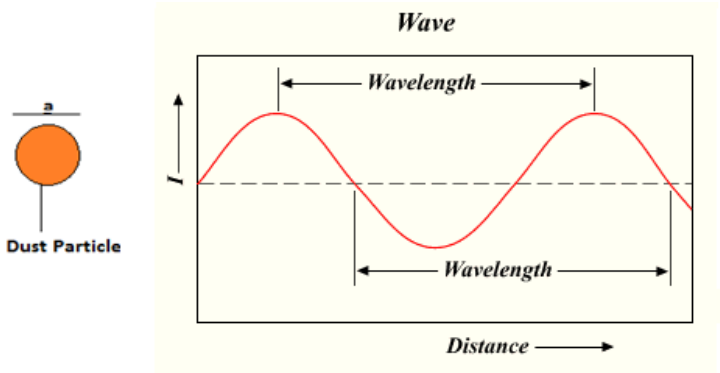

Fig. 4

Mathematically, Interstellar reddening is inversely proportional to the wavelength of incoming light because the equivalent size of dust particles and wavelength, And is given by Color index (i.e. color estimation of an object).

$$i.e.\ 2\pi a = \lambda\ (dust, optical) \Rightarrow Scattering \propto \lambda^{-1}$$

$$E(B\text{-}V)\ [color\ excess] = [instrumental\ color] - [standard\ color]$$

$$E(B\text{-}V) = (B\text{-}V)_i - (B\text{-}V)_o$$

Always shorter
minus longer,
e.g., E(B-V),E(I-K), E(U-B)

To get the value of Interstellar reddening we drew the Color- Color diagram (fig. 5) and then fitted our curve with Standard Color-Color diagram, which gave us the value of reddening to be variable between (~0.59±0.04 mag to ~0.96±0.05 mag) which is in good agreement with previous studies[7].

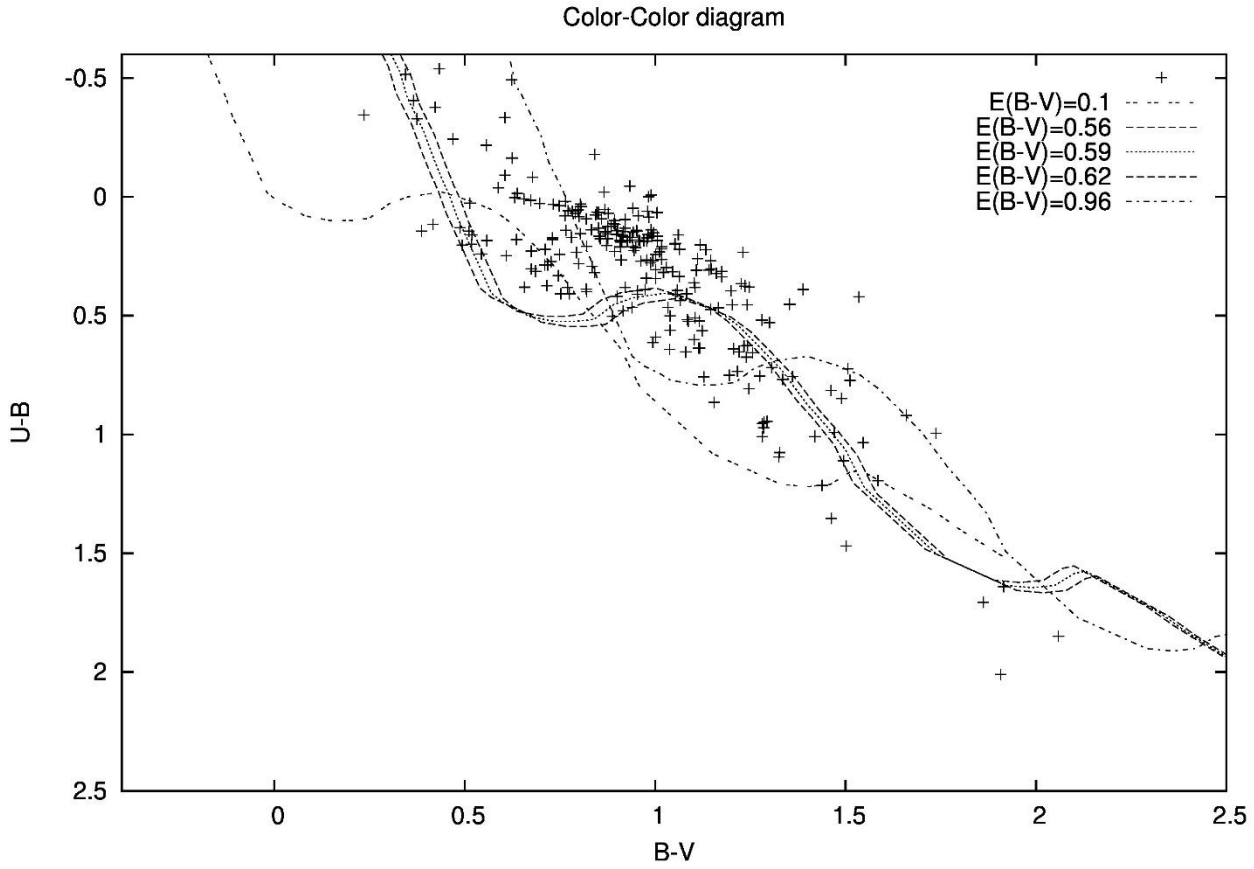

Fig. 5

Color-Color diagram (NGC 1931) for our observations, clearly showing the variable reddening in the star forming region. The ZAMS (Zero-age main-sequence) from Schmidt-Kaler (1982) is shifted along a normal reddening vector having a slope of E(U −B)/E(B−V) = 0.72. Also the comparison of the fit of the Schmidt-Kaler (1982) main –sequence two color curve, reddened by *E(B-V)*=0.56, 0.59 and 0.62, to the observed two-color diagram of NGC 1931.

After estimating the degree of reddening (i.e. E(B-V)) we used equation (10) (true only for our galaxy) to calculate the interstellar extinction (A_v) for our object in V band.

$$\frac{A_V}{E(B-V)} = 3.1 \qquad ---(10)$$

3.2 Distance of the cluster

To find the distance of the cluster we drew the Color-Magnitude diagram (fig. 6), and fitted it with isochrones of (log(age)~ 6.00) (Marigo et al.2008). To fit the isochrones to our stars we used following equations for X and Y shift.

$$\frac{E(V-I)}{E(B-V)} = 1.25 \qquad ---(11)$$

$$\Delta x = (V\text{-}I)_o + 1.25 \cdot E(B\text{-}V) \qquad ---(12)$$

$$\Delta y = V_o + \mu \qquad ---(13)$$

Where μ = Distance Modulus

After estimating the value of distance modulus we used equation (14) to calculate the distance of our cluster in kpc unit.

$$m - M = 5 \cdot \log_{10} D - 5 + A_V \qquad ---(14)$$

Where, m = Apparent magnitude corrected for effects for interstellar extinction.

M = Absolute magnitude of object (i.e. magnitude of object would have been appeared if the object would have been at distance 10 pc).

$m - M$ = distance modulus

D = Distance of object in kilo parsec (kpc).

We got the value for distance modulus as 13.65±0.32, giving us the distance as 2.31±0.34 kpc, which is in good agreement with previous studies [7],[8],[10]. The obtained Color – Magnitude diagram for our observations is shown in fig. 6.

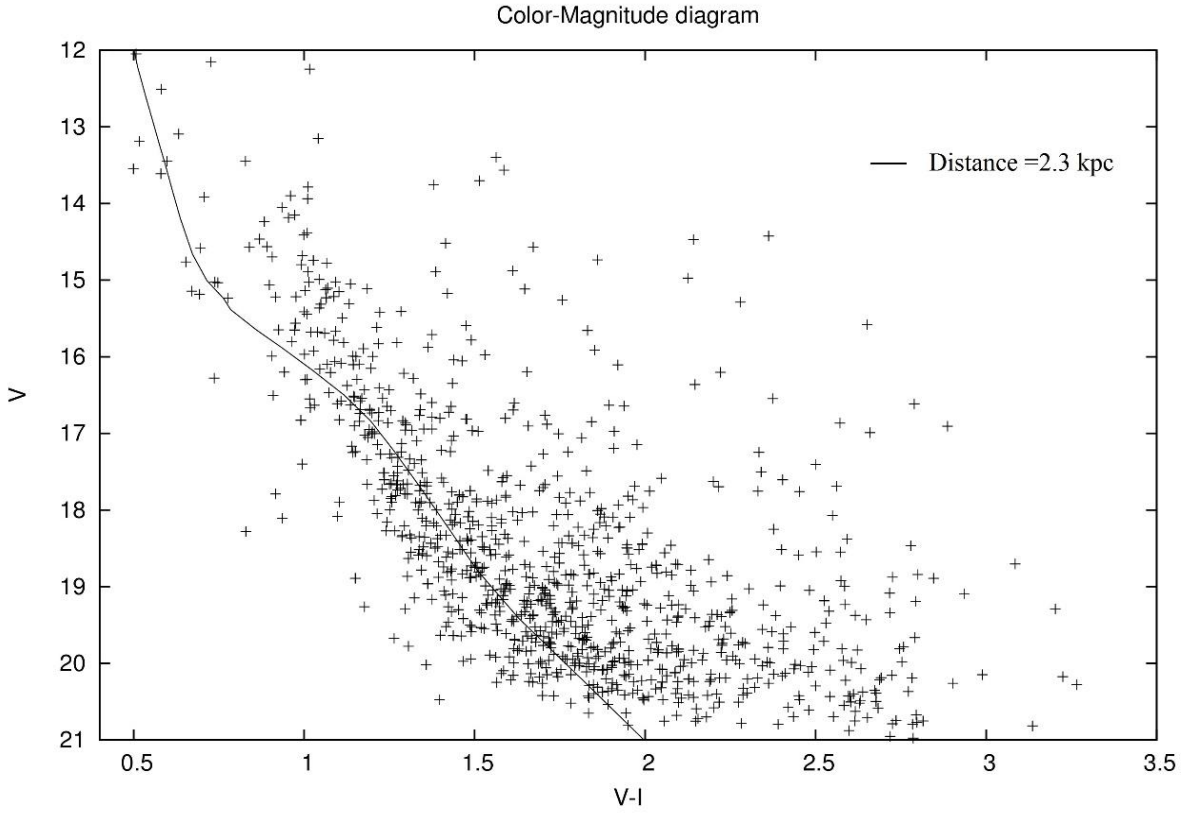

Fig. 6

De-reddened V versus (V-I) CMD for NGC 1931. The post main-sequence isochrones for 1 Myr (Z=0.02) by Marigo et al. (2008) has been plotted after correcting for the distance and reddening.

3.3 Age of the cluster

As from Color-Magnitude diagram it is clear that most of the star members (most massive ones i.e. having less magnitudes means more brighter) lie on the main sequence line of isochrones (log(age) ~6.00) so this is probably a young cluster of about 1-2 Myr[7].

4 Error Analysis

4.1 Interstellar Reddening and Extinction

An estimate of systematic uncertainty in the value of *E(B-V)* is difficult, because these errors arise from uncertainties in the intrinsic colors of the stars. In our error analysis some assumption had been taken (Phelps & Janes, 1994[13]) to make the estimation easy. We used equation 15 to calculate error in reddening and extinction.

$$\sigma^2_{E(B-V)} \sim \sigma^2_{(U-B)} + \sigma^2_{(B-V)} + \sigma^2_{fit} \qquad \text{---(15)}$$

Where $\sigma^2_{E(B-V)}$ = Uncertainty in reddening.

$\sigma^2_{(U-B)}$, $\sigma^2_{(B-V)}$ = Uncertainty in transformation to standard system.

σ^2_{fit} = visual fit error in fitting the standard curve (shown in fig. 5)

Assuming typical values [13] for $\sigma_{(U-B)}, \sigma_{(B-V)}$ as 0.02 and 0.01 respectively (for Landolt system) and $\sigma_{fit} = 0.03$ (from fig. 5),we calculated the error in *E(B-V)* (i.e. $\sigma_{E(B-V)}$) which turned out to be 0.04.

4.2 Distance modulus and Distance

The uncertainty in the true distance modulus, σ^2_{μ} is composed of uncertainties in the apparent distance modulus as well as uncertainties associated with *E(B-V)* (eqn. 12 & 14). We calculated first the error in *E(B-V)* from above analysis and then assuming $\sigma_{ZAMS} = \sigma_{M_v} = 0.3$ mag[13] from equation (16)[13] we estimated the error in distance modulus, μ.

$$\sigma^2_{\mu} = 0.10 + 0.01 \cdot E^2(B\text{-}V) \qquad \text{---(16)}$$

Using $E(B\text{-}V)_{min} = 0.59$, the uncertainty in distance modulus, σ_{μ} turned out to be 0.32.

The uncertainty in the distance, σ_D, is directly related to the uncertainty in the distance modulus by equation 17[13],[14].

$$\sigma_D^2 = \sigma_\mu^2 \cdot \left(\frac{\partial D}{\partial \mu}\right)^2 \qquad \text{---(17)}$$

Now from eqn. 14, eqn. 17 would be reduced to equation 18[13].

$$\sigma_D^2 = 0.213 \cdot D^2 \sigma_\mu^2 \qquad \text{---(18)}$$

where D is in parsec.

Using the calculated values of *D* and σ_μ we estimated the σ_D that turned out to be 0.34.

5 Results and Conclusions

The main aim of the project was to estimate the basic parameters (such as age, distance and reddening) of the cluster and check the consistency of results with previous studies. We found the reddening to be variable (~0.59 ±0.04 mag to ~0.96±0.05 mag) in the star forming region of NGC 1931. This variable reddening shows that the young hot stars are still embedded in the molecular cloud of nebula. The distance modulus turned out to be 13.65±0.32 giving the distance of the cluster to be 2.31±0.34 kpc which is in very good agreement with all previous studies [7],[8],[10].The age was found to be between 1 to 2 Myr using Color-Magnitude diagram showing that most of the stars (including massive ones) lie on the main sequence line of ZAMS curve describing the fact that cluster is young[7].

6 Acknowledgement

The writer is very much grateful to his guide Dr. Saurabh Sharma who inspired him to carry this elegant project and introduced him to the exciting and bright subject of Astronomy. The writer also pays his sincere thanks to Devesh Path Sariya, Sumit Kumar Jaiswal and Ram Kesh Yadav, ARIES for clarifying the doubts while doing photometry. The writer is also grateful to VSPA committee of ARIES to give him this kind opportunity. We are also thankful to NASA Astronomical Database, IRAF and NOAO for all required astronomical software.

References:

[1] Milky Way –Wikipedia

[2] Near- and Mid –IR Photometry of the Pleiades and a New List of Substellar Candidate Members: Stauffer et al., 2007,The ApJ Supplement Series, 172:663-685

[3] Herbig, G. H. 1962, ApJ, 135, 736.

[4] http://www.astro.iag.usp.br/~wilton/file/whatsnew.txt

[5] The age of the oldest Open Clusters: Salaris et al. 2004 Astronomy and Astrophysics, v.414, p.163-174

[6] Widhalm, A. M., and S. Kafka. "WOCS Long-Term Variability in Open Cluster NGC 2141."

[7] Optical Photometric and Polarimetric investigation of NGC 1931: Pandey et al. 2013 ApJ 764 172

[8] Moffat, A. F. J., Jackson, P. D., & Fitzgerald, M. P. 1979, A&AS,38, 197

[9] NGC 1931@SEDS NGC object pages (spider.seds.org/ngc/ngc.cgi?1931)

[10] Pandey, A. K., & Mahra, H. S. 1986, Ap&SS, 120, 107

[11] www.cfht.hawaii.edu/ObsInfo/Standards/Landolt/

[12] Marigo, P., Girardi, L., Bressan, A., Groenewegen, M. A. T.,Silva, L., & Granato, G. L. 2008, A&A, 482, 883

[13] Phelps, Randy L.& Janes, Kenneth A. The ApJ Supplement Series, 90:31-82, 1994 January

[14] Data reduction and error analysis for the physical sciences, Bevington, Philp R. New York: McGraw-Hill, 1969.